Preflight Summary Report for: ECS paper-Revised-2.pdf

Profile: Convert to PDF/A-1b (Processed pages 1 to 14)

Processed by Sophia S, Date: 12/14/20 4:07 PM

Fixups

- Convert to PDF/A-1b (2 objects)
- Force blend color space to sRGB (5 objects)
- Make document XMP Metadata compliant with PDF/A-1 (1 object)
- Remove document structure compression (1 object)
- Compress all uncompressed objects using lossless ZIP compression (1 object)
- Recompress LZW as ZIP (1 object)
- Adjust colors for PDF based ISO standards (1 object)
- Fix font encoding (CIDSet) (6 objects)
- Fix font encoding (CIDToGIDMap) (3 objects)
- Convert SMask to image mask (5 objects)
- Insert missing Type entry in StructElem objects (1224 objects)
- Remove unnecessary transparency groups (5 objects)

Results (Summary)

✓ **No problems found**

Document information

File name: "ECS paper-Revised-2.pdf"
Path: "/Users/sophias/Desktop"
PDF version number: "1.4"
File size (KB): 660.2
Author: "Sophia s"
Creator: "Acrobat PDFMaker 20 for Word"
Producer: "Adobe PDF Library 20.13.106"
Created: "12/14/20 9:06 PM"
Modified: "12/14/20 4:07 PM"
Trapping: "Unknown"
Number of plates: 4
Names of plates: "(Cyan) (Magenta) (Yellow) (Black) "

Environment

Preflight, 18.4.0 (249)
Acrobat version: 20.013
Operating system: macOS 10.16.0

Charge Transport in Additive Modulated Aluminum Chloride Deep Eutectic Solvents (DES)

D. Paterno[a] and S. Suarez[a,b]

[a] Physics Department, Brooklyn College of the City University of New York, Brooklyn, New York 11210, USA
[b] Physics Department, The Graduate Center of the City University of New York, New York, New York 10016, USA

The effect of additives on the aluminum species transports in varying molar ratios of $AlCl_3$ deep eutectic solvents (DES) was studied using EIS conductivity measurements. The amides studied were acetamide, propionamide and butyramide and the molar ratios ranged from 1:1 - 1.7:1 for each $AlCl_3$:amide DES. The additives studied were propylene carbonate (PC) and fluoroethylene carbonate (FEC) in 5wt%. While FEC generally lowered the conductivities, PC appears to shift the reaction equilibrium towards lower $AlCl_3$ concentration. It is possible the fluorine atom on the FEC interacts with the $[AlCl_2(amide)_n]^+$ species, creating stronger interactions that lowers the conductivity. The data displayed non-Arrhenius behavior and were fitted using the Vogel-Fulcher-Tammann equation to reveal dynamic behaviors similar to some pure ILs where the effective inter-conversion between the *trans* and *cis* conformations of the anion facilitated faster ion dynamics. These results can be helpful in modifying DES and similar aluminum solvents for electrolyte applications.

Introduction

The need for safe, low cost, high energy and density storage devices is ubiquitous the world over. Similarly ubiquitous are lithium ion batteries (LIBs) (1-4), due to lithium's low molecular weight and small ionic diameter (1.80 Å) which allows it to deliver about 2.5 times the energy compared to others (lead-acid, nickel-metal hydride, nickel-cadmium) (3). These attributes have been especially fruitful for low temperature portable and selective automotive applications. Despite these advantages, issues such as cost, safety and lithium reserves location exist that make finding alternatives necessary (4-9). Additionally, markets such as commercial vehicles, large-scale storage of renewable energies, lightweight wearable electronics and batteries demand alternative energy sources. Together, these provide the need for implementation of more wide-scale competitive alternative electrochemical energy storage (EES) devices. However, due to the breadth of applications and their respective operational requirements, finding one EES to satisfy all is unrealistic. Instead, niche applications are more likely.

As alternatives to LIBs, researchers have turned to various multivalent ion batteries because of their multiple electron (> 1) transfer capability and one example of this is aluminum ion batteries (AIBs). Aluminum metal offers a three-electron redox property, favorable energy density

(theoretical 2980 mAh/gm compared to lithium's 3860 mAh/gm), low reactivity, easier handling, high cyclability and lower cost compared to lithium. It is also one of the earth's most abundant metal element. The Al-air battery - which is comprised of an Al anode, air cathode and suitable electrolyte - has a theoretical voltage of 2.7 V and energy density of 8.1 kWh/kg, and is being considered for future large-scale applications (10-12). Unfortunately, Al has a high open-circuit potential (-1.66 V vs. a standard Hg/HgO with a 4M NaOH electrolyte at 25°C) (13), which prevents the use of highly conducting aqueous electrolytes due to the decomposition of water before deposition of Al. Additionally, Al has a strong affinity towards oxygen and hence cannot be electrolyzed from aqueous solutions (14). Most detrimental is the formation of protective oxide layers on the surface of Al which despite providing excellent corrosion resistance, also prevents the use of Al as an anode material. This oxide layer cannot be dissolved in most aqueous electrolyte solutions. However, high temperature molten salts have provided some aid with this problem (7), but due to their high working temperatures and cost, alternatives are needed.

The selection of the electrolyte is very important in batteries as they must allow the transports of ionic species between the electrodes while simultaneously blocking that of electrons. In the case of AIBs, chloroaluminate ILs have been used in aluminum electrodeposition (15-17) and because of their relatively high ionic conductivity, tunable acidity, and wide electrochemical window, to date they are the most used electrolytes in AIBs. Chloroaluminate ILs exhibit Lewis acid-base behavior with the solution pH, speciation and reactivity being determined by the chloride donor's concentration. They are mixtures of ionic liquids such as dialkylimidazolium chloride and metal halide salts of which the most used is aluminum chloride ($AlCl_3$) (18-25). The acidic $AlCl_3$/[EMIm]Cl system have received the most attention and depending on the molar ratio of $AlCl_3$ to the imidazolium chloride the electrolyte can be classified as basic (<1), acidic (>1) and neutral (=1). The different anionic species present in the basic melt are $AlCl_4^-$ and Cl^-, in acidic $Al_2Cl_7^-$, and $AlCl_4^-$ in neutral solution (18-29). The electrochemical reduction of $Al_2Cl_7^-$ ion in acidic solution proceeds as (26, 28, 30-32):

$$4\ Al_2Cl_7^- + 3e^- \rightarrow Al + 7\ AlCl_4^- \qquad [1]$$

Recently, deep eutectic solvents (DES) (33-40) have gained attention as electrolytes for energy storage devices (34-37). Fundamentally they are comprised of ionic and non-ionic moieties, with thermal and physical properties that are similar to room temperature ionic liquids. They are however generally cheaper and easier to prepare, and are also known to dissolve metal oxides (41) - which is one of the reasons for our interest. The reactions of DESs depend on several factors including the metal atom, the presence of chlorine coordinated cations or anions, and the hydrogen bond donor. In the case of metal halides, the eutectic formation rests with their asymmetric splitting whereby anions and donor-coordinated cations are formed (33). For $AlCl_3$, this process results in the formation of anionic and cationic structures such as $AlCl_4^-$, $Al_2Cl_7^-$, and $[AlCl_2(amide)_n]^+$ structures where n = 1 and 2 (33). Examples of possible equilibria are presented in Eqs. 2-4 (36) where L represents the amide.

$$2[AlCl_3L_n] \leftrightarrow [AlCl_2L_n]^+ + [AlCl_4]^- + nL \qquad [2]$$

$$2[AlCl_3L_n] + Al_2Cl_6 \leftrightarrow 2[AlCl_2L_n]^+ + 2[AlCl_4]^- \quad [3]$$

$$2[AlCl_4]^- + Al_2Cl_6 \leftrightarrow 2[Al_2Cl_7]^- \quad [4]$$

At low molar ratios, reaction 2 is favored. With increasing $AlCl_3$ concentration, the equilibrium shifts to reaction 3, and finally at higher molar ratios reaction 4 becomes the norm. Like ionic liquids, the transport properties of DESs can be tuned. Changing the hydrogen bond donor or the metal atom will change the resulting DES properties. Including additives can also change these properties. An example of this is the 1.3:1 molar ratio $AlCl_3$:Urea DES prepared by Yu et.al. (34) incorporating the 1,2-dichloroethane (DCE) additive. The pure DES ^{27}Al NMR spectrum was broad and extended between 95 and 105 ppm, while the additive DES gave individual peaks, possibly suggesting that either the additive reduced the electrostatic interactions between neighboring ions, or that it aided in moving the equilibrium reaction more in favor of ionic species.

In an effort to improve the ion transports in DES electrolytes, we have embarked on a series of studies that are focused on elucidating the various aluminum ion species and the interactions that govern their dynamics. Our initial study (42) delved into the local dynamics of the pure DES electrolytes comprised of varying molar ratios (1:1 – 1.7:1) of $AlCl_3$ mixed with acetamide (AA, AcA), butyramide (BA, BuA), or propionamide (PA, PrA). Our goal was to determine how the aluminum ion transport and speciation were affected by the amide type, relative concentration and temperature. We used ^1H and ^{27}Al Nuclear Magnetic Resonance (NMR) spin-lattice relaxation times, chemical shifts and linewidth measurements, complimented with electrochemical impedance spectroscopy (EIS) ionic conductivity measurements, both as a function of temperature. The amides were chosen because they differ in the alkyl chain length which may help in elucidating their electron donor capabilities and the resulting aluminum ion species formed. Our variable temperature conductivity results (42) showed a non-Arrhenius behavior which was fitted using the Vogel-Fulcher-Tammann (VFT) equation. Generally, VFT behavior indicates a 'fragile' state (43), where dynamics are the result of available free volume and disorder resulting from molecular fluctuations and reorganizations over a wide variety of different particle orientations and coordination states, almost independently of thermal aid. Unlike the case for the typical EMIM[Cl] ionic liquid, there was no monotonic decrease in the T_o value with increasing $AlCl_3$ concentration for any of the amides. Similarly, the pseudo activation energy did not display a monotonic increase with increasing $AlCl_3$ concentration. These indicate a significant difference between the ionic environments of the $AlCl_3$ DES analogues compared to the ionic liquid systems.

In this study we continue the characterization of the DES dynamics by focusing exclusively on the effect of the inclusion of additives such as propylene carbonate (PC) and fluoroethylene carbonate (FEC) on the transport of the aluminum species. Additives such as propylene carbonate (PC, dielectric constant 64.92 at 25°C, 132°C flash point, melting point -49°C) have been used in lithium ion battery electrolytes to reduce solution viscosity and enhance ion dynamics (44-47). FEC (48) has also been used but as a stabilizing additive for PC, thereby enhancing the electrolyte's cycling stability and solid electrolyte interface (SEI) formation capability. In our

efforts to not only improve the dynamics of the DES electrolytes for AIB applications, we incorporated each into the pure DESs. We expect their inclusion to provide additional hydrogen bonding pathways for the aluminum ion species, which can affect the resulting ion transport. Towards this, we report for the first time variable temperature ionic conductivity measurements of varying molar ratios (1:1 – 1.7:1) of $AlCl_3$:amide (acetamide, propionamide, and butyramide) with 5wt% PC, or FEC additives. Our future publications will include EIS measurements for additional additives and concentrations, and the comprehensive viscosity and NMR analyses of all DESs.

Experimental

Sample Preparation

The electrolytes studied were varying concentrations of the amides: acetamide (AA, AcA, CH_3CONH_2, Alfa Aesar, > 99%), butyramide (BA, BuA, $CH_3CH_2CH_2CONH_2$, Frontier Scientific, > 99%), and propionamide (PA, PrA, $CH_3CH_2CONH_2$, Frontier Scientific, 99%), with Aluminum chloride ($AlCl_3$, Alfa Aesar, > 99%). The additives used were 5wt% fluoroethylene carbonate (FEC, Sigma-Aldrich, anhydrous, 99%) and propylene carbonate (PC, Sigma-Aldrich, anhydrous, 99%). Chemical structures of these amides are shown in Figure 1. The amides were dried in a vacuum oven at 353K for 40 hours while the $AlCl_3$ was used as received. Both $AlCl_3$ and the amides were combined in their appropriate masses to create the required molar ratios of mixtures, which were mixed slowly with a magnetic stirrer to form the resulting liquid. The required amounts of additives were then added to the respective DES, after which the mixture was heated and magnetically stirred at 80ºC for an additional 36 hours. The work was done in a glove box under constant flowing nitrogen atmosphere. The exothermic nature of the reaction eliminated the need for heating or vigorous mixing.

EIS Ionic Conductivity

Solvents were packed in a dry nitrogen atmosphere into an airtight 3 mL (Biologic Brand) two-electrode sample cell, leaving 50% of the cell volume available for thermal expansion. The cells were temperature controlled from 303 to 363K using a silicone oil bath. The electrochemical impedance measurements were done using a Solartron 1260 Impedance Analyzer coupled with a Solartron 1287 Electrochemical Interface. Experimental parameters utilized a frequency sweep from 25 Hz to 2.5 MHz using a resolution of 20 data points per decade and the energization was set with AC amplitude of 10 mV with no DC offset. The resulting Nyquist plot of reactance versus resistance was inspected to determine the real electrical resistance. Using the corresponding cell constants and the electrical resistance, conductivity was calculated and plotted versus temperature. Data shown and discussed are the averages of three sets of measurements.

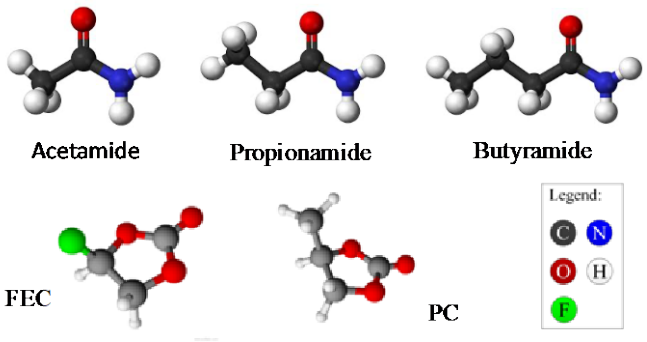

Figure 1. Chemical structures for the amides and additives.

Results

Variable temperature EIS ionic conductivity data were determined for $AlCl_3$:amide (acetamide, butyramide and propionamide) DESs with 5wt% propylene carbonate (PC) or fluoroethylene carbonate (FEC) additive. Conductivity (σ) values were obtained from corresponding Nyquist plots. The general behavior of the conductivity was a dependence on molar concentration, temperature, additive and amide types. Generally, several factors can contribute to σ but usually the biggest contributors are temperature, solution viscosity and the number of available charge carriers. We see the relationships between these parameters through the Nernst-Einstein (NE, left) and Stokes-Einstein (SE, right) equations (Eq. 5-6):

$$\sigma = \frac{Dq^2c}{k_BT} \quad [5]$$

$$D = \frac{k_BT}{4\pi r\eta} \quad [6]$$

where η, D, q, k_B, c, T and r are the solution viscosity, self-diffusion coefficient, charge of the carrier, Boltzmann constant, charge carrier concentration, temperature in Kelvin, and hydrodynamic radius respectively. Ideally, both equations are for application to very dilute solutions where the ions are depicted as hard non-interacting spheres, moving through a continuum of viscosity η. Correspondingly, the ions are expected to be single entities. Because of these, large errors are often obtained from the application of either equation to concentrated systems. The main sources of errors are usually due to concentration, relaxation or drag, and electrophoretic effects.

Temperature and Concentration Effects

As shown in Figure 2 for $AlCl_3$:PA (propionamide) with 5wt% FEC (left) and 5wt% PC (right), the conductivity increased with increasing temperature. This behavior was also observed for the $AlCl_3$:AA-additive and $AlCl_3$:BA-additive mixtures, as well as for the pure DESs (42). The increase in conductivity with temperature is expected since the greater thermal energies will cause

reduced electrostatic interactions resulting in faster ion dynamics. There was a maximum in σ for all DES-additive mixtures. For both the $AlCl_3$:PA and $AlCl_3$:BA, the maximum for the 5wt% PC mixtures occurred at the 1.1:1 molar ratio, while for the $AlCl_3$:AA mixture it occurred for the 1.5:1 molar ratio for all temperatures. In the case of the 5wt% FEC, the maxima occurred at the 1.3:1 molar ratio for all three amide mixtures. For comparison sake, the maxima for the pure $AlCl_3$:PA and $AlCl_3$:BA DES electrolytes occurred prominently at the 1.3:1 molar ratio (42) for all temperatures. The pure $AlCl_3$:AA DES had a broad plateau starting at the 1.1:1 molar ratio at lower temperatures which gave way to a more pronounced maximum at the 1.3:1 molar ratio at higher temperatures (42).

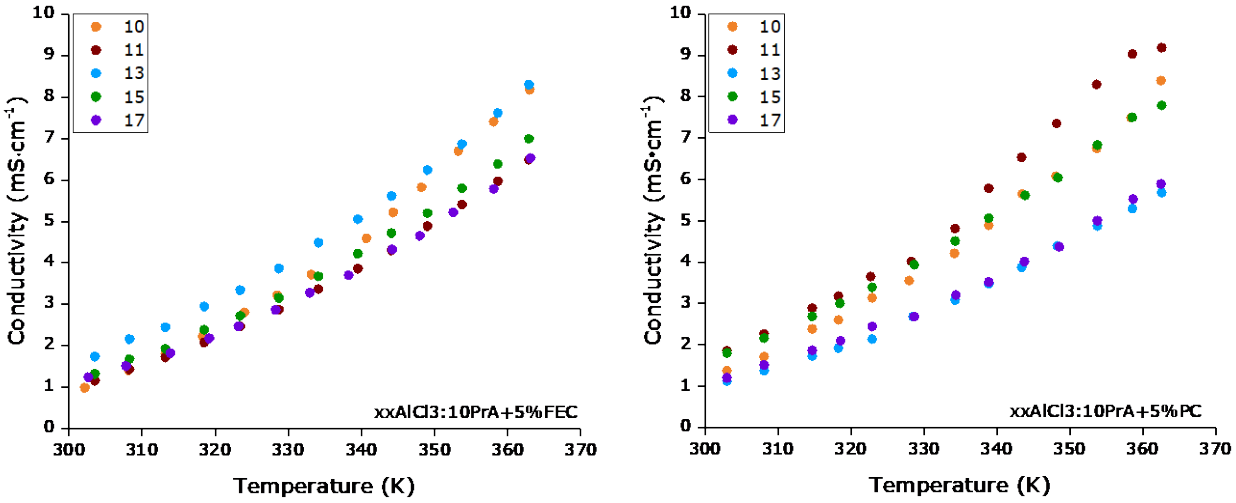

Figure 2. Variable temperature ionic conductivity data for varying molar ratios of $AlCl_3$:PA (propionamide) with 5wt% FEC (left) and 5wt% PC (right).

Like the pure DES, the maximum in conductivity may be due to a combination of factors. As shown in the NE equation, the increasing ionic species associated with greater $AlCl_3$ concentrations can increase the conductivity. Generally, an increase in charge concentration is accompanied by similar increases in viscosity. Unfortunately, we did not perform viscosity measurements on either the pure or additive mixtures but those measurements are a part of our future studies. We used the viscosity results of Liu et. al. (49) for the pure DESs - which for acetamide showed a linear decrease with increasing molar ratio, but for both the propionamide and butyramide DES electrolytes exhibited a broad minimum between 1.1:1 and 1.3:1 molar ratios. Since the minimum in η coincides with the maximum in σ for both the propionamide and butyramide additive mixtures, it suggests that viscosity is still influencing their aluminum ion transports. The additive dependent maximum in conductivity also supports the additive type being used as an additional tuning parameter for DES electrolytes and suggests differences in the interactions between the amides, the aluminum species and the additives.

Amide and Additive Type Effects

The effect of the additive type on the conductivity of the $AlCl_3$:amide-additive mixtures is illustrated more clearly in Figures 3 and 4 for the 1.1:1 (left) and 1.5:1 (right) molar ratios of $AlCl_3$:amide-additive mixtures. As shown in Figure 3, the 5wt% PC additive increased the conductivity for the 1.1:1 $AlCl_3$:PA, 1.1:1 $AlCl_3$:BA, 1.5:1 $AlCl_3$:AA and 1.5:1 $AlCl_3$:BA analogues compared to their pure forms. Similar enhancements were observed for the 1:1 $AlCl_3$:PA and 1.7:1 $AlCl_3$:AA analogues. As shown in Figure 4 for the 5wt% FEC mixtures, generally no enhancement was observed for the FEC mixtures and this was the trend for all molar ratios and amide types. Both FEC (78.4 at 25ºC) (48) and PC (64.92 at 25ºC) (44-47) have high dielectric constants and should offer additional screening for the aluminum species. Whereas the PC can serve as a solvent for LIB electrolytes and is often used in greater quantities than 5wt%, the FEC is used to enhance the electrolyte's SEI formation capability and cyclability and is used in similarly small quantities. Since the DES solvents are the potential electrolytes for AIBs, any additive incorporated is expected to be used in small quantities, therefore the 5wt% of both PC and FEC seems appropriate. Our future studies will include a variation on the additive concentration as well.

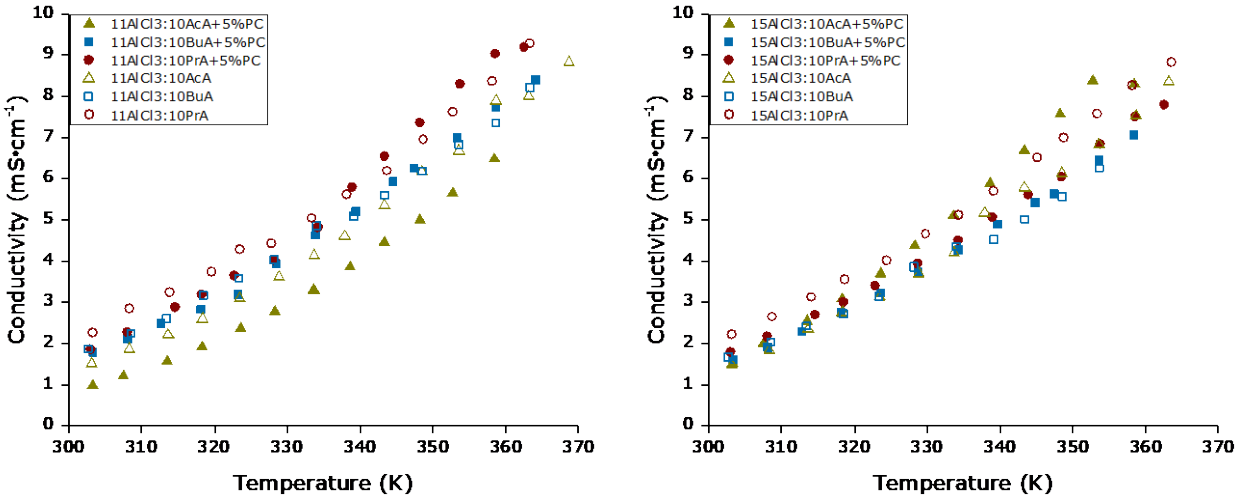

Figure 3. Variable temperature ionic conductivity data for 1.1:1 (left) and 1.5:1 (right) molar ratios of $AlCl_3$:amide-PC mixtures.

The difference between the effect of the two additives may be based upon their structures. As shown in Figure 1, the FEC additive has a terminating fluorine atom while PC has a methyl group. Unlike the methyl group, the terminal fluorine atom can interact electrostatically with the aluminum cationic $[AlCl_2(amide)_n]^+$ species. This has been shown in LIB electrolytes such as $LiPF_6$/EC/DEC/FEC where the FEC enhanced the formation of LiF (50) over Li_2CO_3. This interaction would result in stronger local interactions between the aluminum species and their solvation spheres thereby resulting in reduced transports and lower ionic conductivities. Unlike FEC, PC selectively enhances the mixtures ionic conductivity. Although preliminary, it appears PC shifts the reaction equilibrium to favor lower molar ratios for both propionamide and butyramide. In the case of acetamide, in spite of the concentration at which the conductivity maximum occurs remaining unchanged, the fact that the maximum encompassed the entire

temperature range - unlike for the pure DES - suggests PC reduced the electrostatic interactions between the aluminum species.

To determine the effect of the amide type on the conductivity we compared their structure. The size of the amide molecules is as follows: BA>PA>AA (see Figure 1). Compared to both propionamide and acetamide, butyramide is most bulky and because of this, its interaction with the various ionic species could be less effective. The effect of amide size seems to be temperature and concentration dependent. For PC additive mixtures, at molar ratios above 1.1:1 and temperatures below 343K, the acetamide mixtures have the lowest conductivity. Above this temperature the trend reversed. Additional revelations include propionamide mixtures at the 1:1 and 1.1:1 molar ratios being most conducting, while the butyramide were slightly more than the acetamide. This behavior was also observed for the pure DESs (42). For the FEC additive, generally acetamide mixtures have the lowest conductivities below 353K, while above they have the highest and also the largest thermal enhancements.

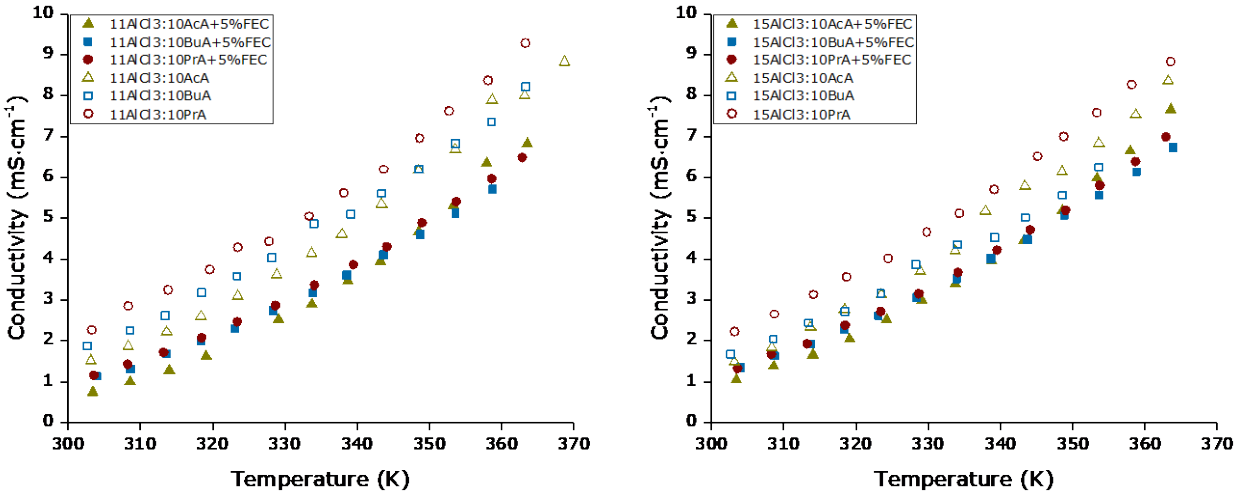

Figure 4. Variable temperature ionic conductivity data for 1.1:1 (left) and 1.5:1 (right) molar ratios of $AlCl_3$:amide-FEC mixtures.

The high-temperature thermal enhancements in conductivity experienced by the acetamide mixtures suggest the breaking of the hydrogen bonding network. Generally, hydrogen bonds lessen in strength and connectivity with increasing temperature. This can lead to faster ion dynamics as a result of the reduced interactions. Since the strength of the hydrogen bonding network as well as the local electrostatic interactions are modulated by the dielectric screening of the amide molecules, we tried to compare their dielectric constants. Unfortunately, at the time of writing only acetamide had a publicly available dielectric constant. Values were however available for their N-methyl analogues which at 30°C are: 178.9, 164.3 and 124.7 respectively for N-methylacetamide (51-52), N-methylpropionamide (53-54) and N-methylbutyramide (55). N-methylacetamide having the highest dielectric constant could support the acetamide mixtures having lower conductivities. The N-methylbutyramide analogue having the lowest dielectric constant could support butyramide providing a weaker hydrogen bonding network. However, as previously stated, due to butyramide's bulky size, its solvating properties and the resulting ion dynamics in its

mixtures may be further impeded. Also, in the case of butyramide the inclusion of the PC molecules seems to provide additional screening for the aluminum species which allows for faster ion dynamics. This suggests that amide size is a determining factor as it affects the resulting electrostatic interactions between the ionic species, as well as their mobilities. Whereas the acetamide appears too small to provide effective screening for the aluminum species especially at lower temperatures, the butyramide appears too bulky to provide efficient translational dynamics at higher temperatures. The propionamide however appears to balance effectively the need for effective electrostatic screening and translational dynamics.

The inverse temperature behavior of the logarithmic conductivity was fitted to the VFT equation:

$$\sigma = \sigma_o \exp\left(\frac{-B}{T - T_o}\right) \quad [7]$$

where the adjustable parameters - B, T and T_o - are the pseudoactivation energy, current temperature, and 'pseudo' ideal glass transition temperature respectively in unit of Kelvin. The logarithmic form of the VFT was used instead of the exponential as it allows better fitting of data spanning orders of magnitude. Additionally, when compared to the Arrhenius fit, the VFT produced smaller errors and had R^2 values greater than 0.99 indicating the VFT was a more suitable model. As previously mentioned, the pure DESs also had curve-like inverse temperature behavior of their logarithmic conductivities and were fitted using the VFT equation (42). A representative plot for the variable molar ratios $AlCl_3$:AA DES with 5wt% FEC (left) and 5wt% PC (right) additives are shown in Figure 5. Similar behaviors were observed for the $AlCl_3$:PA-additive and $AlCl_3$:BA-additive mixtures (both not shown). There is no data for the 1:1 $AlCl_3$:AA and 1.7:1 $AlCl_3$:BA with 5wt% PC because the additive caused precipitation of the mixture.

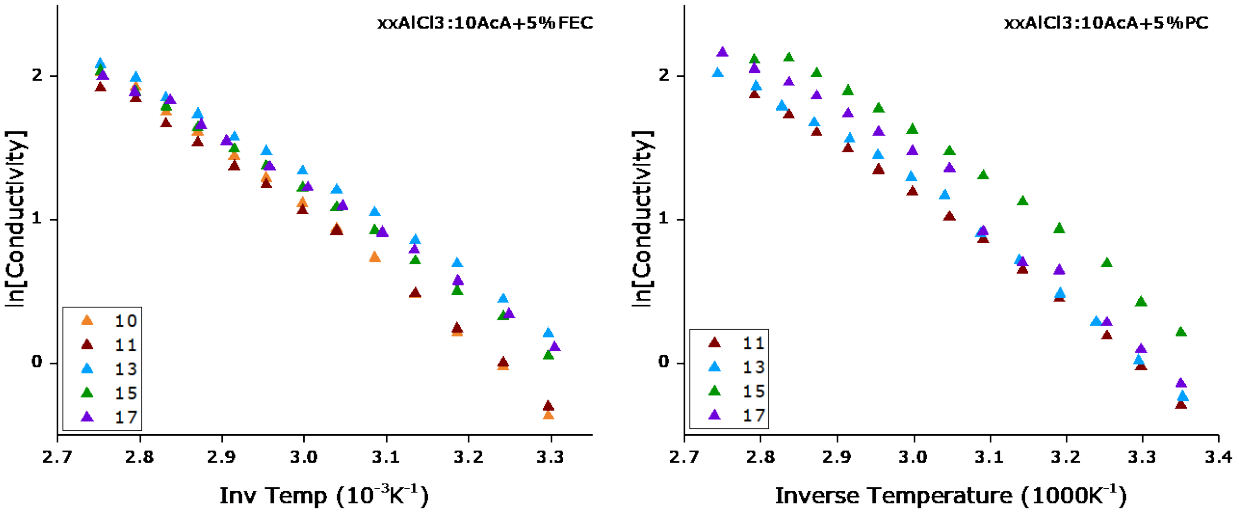

Figure 5. VFT plots of the ionic conductivity for 5wt % FEC (left) and 5wt % (right) $AlCl_3$:AA DES electrolytes.

As previously stated, liquids displaying VFT behaviors are dynamically disordered on the molecular level, whereby species reorganize over a wide variety of different particle orientations and coordination states, without thermal aid. The Fragility (*F*) value is generally accepted as an indicator of this dynamic behavior and values for both $AlCl_3$:amide-additive mixtures were determined from the relationship: B/T_o. *F* is used instead of *D* to differentiate the Fragility parameter from the self-diffusion coefficient (*D*) which is depicted in the SE equation and is part of our future studies. As shown in Tables I and II, the Fragility values range from 3.7 to 9.4. Generally, fragility values for most ILs fall between 5 and 10. Those with values below 5 are considered 'most fragile.' This was demonstrated by Castner et.al. (56) in their study of the effect of the symmetry of fluorinated anions on dynamics in imidazolium based ILs. They obtained a value of 3.80 for the 1-ethyl-3-methylimidazolium bis(trifluoromethylsulfonyl)imide IL and attributed this to the effective inter-conversion between the *trans* and *cis* conformations of the anion that facilitated faster ion dynamics.

Table I. VFT fitting parameters for the 5wt% PC in varying molar ratio $AlCl_3$:amide DES electrolytes. Pseudo-activation energies (*B*) are given in Kelvin but can be represented in kJ/mol using the conversion factor 1kJ/mol = 120.31 K. Corresponding Arrhenius activation energies (E_A) and Fragility (*F*) are also included.

	T_0	*B*	*F*	E_A
Sample	(K)	(K)		($kJ \cdot mol^{-1}$)
10AlCl3:10AcA+5%PC				
11AlCl3:10AcA+5%PC	181 ± 4	743 ± 40	4.1 ± 0.1	6.2 ± 0.1
13AlCl3:10AcA+5%PC	227 ± 9	497 ± 78	2.2 ± 0.1	4.1 ± 0.1
15AlCl3:10AcA+5%PC	182 ± 19	666 ± 187	3.7 ± 0.2	5.5 ± 0.2
17AlCl3:10AcA+5%PC	158 ± 34	1037 ± 438	6.6 ± 0.4	8.6 ± 0.4
10AlCl3:10BuA+5%PC	192 ± 10	502 ± 76	2.6 ± 0.1	4.2 ± 0.1
11AlCl3:10BuA+5%PC	187 ± 16	546 ± 129	2.9 ± 0.1	4.5 ± 0.1
13AlCl3:10BuA+5%PC	191 ± 5	489 ± 33	2.6 ± 0.1	4.1 ± 0.1
15AlCl3:10BuA+5%PC	195 ± 5	477 ± 37	2.4 ± 0.1	4.0 ± 0.1
17AlCl3:10BuA+5%PC				
10AlCl3:10PrA+5%PC	207 ± 8	447 ± 59	2.2 ± 0.1	3.71 ± 0.06
11AlCl3:10PrA+5%PC	144 ± 31	961 ± 321	6.7 ± 0.1	8.0 ± 0.1
13AlCl3:10PrA+5%PC	164 ± 13	757 ± 118	4.6 ± 0.1	6.3 ± 0.1
15AlCl3:10PrA+5%PC	182 ± 5	544 ± 40	3.0 ± 0.0	4.53 ± 0.04
17AlCl3:10PrA+5%PC	171 ± 14	667 ± 119	3.9 ± 0.1	5.5 ± 0.1

Compared to the Fragility values of the pure DESs, those for the $AlCl_3$:amide-additive mixtures are larger. Depending on the molar concentration, the pure DES is expected to contain anionic ($AlCl_4^-$, $Al_2Cl_7^-$), cationic ($[AlCl_2(amide)_n]^+$) and neutral ($[AlCl_3(amide)]$ and $[AlCl_3(amide)_2]$) aluminum species. The inclusion of the PC additive is not expected to alter these species. However, the FEC can cause the formation of additional species including $[AlCl_2(amide)_n]$ [F]. In spite of this, the relatively small fragility factors support the existence of local conformational changes of the various species. In our future studies which includes ^{27}Al NMR measurements, one of the objectives will be to determine if additional aluminum ion species are formed from FEC and similar fluorinated additives.

Table II. VFT fitting parameters for the 5wt% FEC in varying molar ratio $AlCl_3$:amide DES electrolytes. Pseudo-activation energies (B) are given in Kelvin but can be represented in kJ/mol using the conversion factor 1kJ/mol = 120.31 K. Corresponding Arrhenius activation energies (E_A) and Fragility (F) are also included.

	T_0	B	F	E_A
Sample	(K)	(K)		(kJ·mol^{-1})
10AlCl3:10AcA+5%FEC	195 ± 8	730 ± 83	3.7 ± 0.1	6.1 ± 0.1
11AlCl3:10AcA+5%FEC	193 ± 10	704 ± 104	3.7 ± 0.1	5.9 ± 0.1
13AlCl3:10AcA+5%FEC	180 ± 11	701 ± 106	3.9 ± 0.1	5.8 ± 0.1
15AlCl3:10AcA+5%FEC	162 ± 12	927 ± 135	5.7 ± 0.1	7.7 ± 0.1
17AlCl3:10AcA+5%FEC	161 ± 18	903 ± 190	5.6 ± 0.2	7.5 ± 0.2
10AlCl3:10BuA+5%FEC	163 ± 15	754 ± 139	4.6 ± 0.1	6.3 ± 0.1
11AlCl3:10BuA+5%FEC	197 ± 10	519 ± 76	2.6 ± 0.1	4.3 ± 0.1
13AlCl3:10BuA+5%FEC	150 ± 12	855 ± 118	5.7 ± 0.1	7.1 ± 0.1
15AlCl3:10BuA+5%FEC	187 ± 4	557 ± 34	3.0 ± 0.1	4.63 ± 0.03
17AlCl3:10BuA+5%FEC	126 ± 12	1126 ± 127	8.9 ± 0.1	9.4 ± 0.1
10AlCl3:10PrA+5%FEC	208 ± 6	503 ± 48	2.4 ± 0.1	4.2 ± 0.0
11AlCl3:10PrA+5%FEC	190 ± 3	576 ± 25	3.0 ± 0.1	4.8 ± 0.0
13AlCl3:10PrA+5%FEC	161 ± 13	746 ± 115	4.6 ± 0.1	6.2 ± 0.1
15AlCl3:10PrA+5%FEC	189 ± 10	550 ± 79	2.9 ± 0.1	4.6 ± 0.1
17AlCl3:10PrA+5%FEC	151 ± 7	887 ± 73	5.9 ± 0.1	7.4 ± 0.1

Summary

We determined the variable temperature ionic conductivities for mixtures comprised of varying molar ratios (1:1 – 1.7:1) of $AlCl_3$:amide (acetamide, propionamide, and butyramide) with 5wt% PC, or FEC additives. This was done in an effort to determine the effect of additives commonly

used to improve the performance and ion dynamics of lithium ion battery electrolytes on $AlCl_3$ deep eutectic solvents (DESs). Although the FEC has a larger dielectric constant compared to PC, compared to the pure DES electrolytes the conductivity of the mixtures was generally lowered by the FEC additive but selectively improved by the PC. The smaller conductivities of the FEC mixtures may be due to its terminating fluorine atom which may be interacting with the cationic species to create $[AlCl_2(amide)_n]^+$ [F]. Our future ^{27}Al NMR studies will investigate this possibility, as well as determine the changes in the local dynamics due to the incorporation of the additives. Similar to the pure DES, the $AlCl_3$:amide-additive mixtures show a maximum in conductivity that was amide dependent. In the case of PC, the maximum shifted from 1.3:1 in the pure DES to 1.1:1 molar ratio for both the propionamide and butyramide mixtures. This suggests that for both amides, it is possible to get effective ion transports at lower $AlCl_3$ concentration. Overall, these results show the use of additives can be used to improve and tune the ionic conductivity of deep eutectic solvents for aluminum electrolyte applications, and possibly extend to other multivalent ion electrolytes.

Acknowledgement

This work was supported by the National Science Foundation, Solid State and Materials Chemistry Program, Division of Materials Research, EAGER award # 1841398.

References

1. M. Armand and J.-M. Tarascon, *Nature*, **451**, 652 (2008).
2. H. Chen, M. Armand, M. Courty, M. Jiang, C.P. Grey, F. Dolhem, J.M. Tarascon, and P. Poizot, *J. Am. Chem. Soc*., **131**, 8984 (2009).
3. B. Dunn, H. Kamath, and J.M. Tarascon, *Science*, **334**, 928 (2011).
4. K. Hayamizu, S. Tsuzuki, S. Seki, K. Fujii, M. Suenaga, and Y. Umebayashi, *J. Chem. Phys*., **133**, 194505 (2010).
5. K. Ueno, J.-W. Park, A. Yamazaki, T. Mandai, N. Tachikawa, K. Dokko, and M. Watanabe, *J. Phys. Chem. C*., **117**, 20509 (2013).
6. B. Geĺinas, M. Natali, T. Bibienne, Q. P. Li, M. Dollé, and D. Rochefort, *J. Phys. Chem. C*., **120**, 5315 (2016).
7. H.-T. Kim, J. Kang, J. Mun, S. M. Oh, T. Yim, and Y. G. Kim, *ACS Sust. Chem. Eng*., **4**, 497 (2016).
8. M. L. Phung Le, F. Alloin, P. Strobel, J.-C. Lepretre, C. P. del Valle, and P. Judeinstein, *J. Phys. Chem. B*, **114**, 894 (2010).
9. F. Castiglione, E. Ragg, A. Mele, G.B. Appetecchi, M. Montanino, and S. Passerini, *J. Phys. Chem. Lett*., **2**, 153 (2011).
10. W. Gai and Z.Y. Deng, *J. Power Sources*, **245**, 721 (2014).
11. Q. Li and N. J. Bjerrum, *J. Power Sources*, **110**, 1 (2002).
12. D.R. Egan, C.P. Leon, R. J. K. Wood, R. L. Jones, K. R. Stokes, and F. C. Walsh, *J. Power Sources,* **236**, 293 (2013).
13. M.L. Douche, J.J. Rameau, R. Durand, and F. Novel-Cattin, *Corros. Sci*., **41**(4), 805 (1999).

14. M. Zhang, V. Kamavarum and R.G. Reddy, *JOM*, **55**, 54 (2003).
15. Y.G. Zhao, and T.J. VanderNoot, *Electrochim. Acta,* **42**, 3 (1997).
16. T. Jiang, M.J.C. Brym, G. Dube, A. Lasia, and G.M. Brisard, *Surf. Coat. Technol*., **201**, 1 (2006).
17. T. Jiang, M.J.C. Brym, G. Dube, A. Lasia, and G.M. Brisard, *Surf. Coat. Technol.,* **201**, 10 (2006).
18. J.J. Auborn and Y.L. Barberio, *J. Electrochem. Soc*., **132**, 598 (1985).
19. P.R. Gifford, *J. Electrochem. Soc.*,**135**, 650 (1988).
20. F.M. Donahue, S.E. Mancini, and L. Simonsen, *J. Appl. Electrochem*., **22**, 230 (1992).
21. C.J. Dymek, *J. Electrochem. Soc*., **131**, 2887 (1984).
22. P.R. Gifford, *J. Electrochem. Soc*.,**134**, 610 (1987).
23. R.T. Carlin, J. Fuller, W.K. Kuhn, M.J. Lysaght, and P.C. Trulove, *J. Appl. Electrochem.*, **26**, 1147 (1996).
24. G. Yue, S. Zhang and Y. Zhu, *AIChE Journal*, **55**, 783 (2009).
25. S.J. Ahn, K. Jeong, and J.J. Lee, *Bull. Korean Chem. Soc*., **30**, 233 (2009).
26. P. Rolland and G. Mamantov, *J. Electrochem. Soc*., **123**, 1299 (1976).
27. J. Robinson and R.A. Osteryoung, *J. Electrochem. Soc*., **127**, 122 (1980).
28. P.K. Lai and M. Skyllas-Kazacos, *J. Electroanal. Chem.*, **248**, 431 (1988).
29. T.J. Melton, J. Joyce, J.T. Maloy, J.A. Boon, and J.S. Wilkes, *J. Electrochem. Soc*., **137**, 3865 (1990).
30. R.T. Carlin, W. Crawford, and M. Bersch, *J. Electrochem. Soc*., **139**, 2720 (1992).
31. K.V. Kravchyk, S. Wang, L. Piveteau, and M.V. Kovalenko, *Chem. Mater*., **29**, 4484 (2017).
32. M. L. Agiorgousis, Y.Y. Sun, and S.B. Zhang, *ACS Energy Lett*., **2**, 689 (2017).
33. H.M.A. Abood, A.P. Abbott, A. D. Ballantyne, and K.S. Ryder, *Chem. Commun*., **47**, 3523 (2011).
34. W. Chu, X. Zhang, J. Wang, S. Zhao, S. Liu, and H. Yu, *Energy Storage Mater.*, **22**, 418 (2019).
35. B. Guchhait, S. Das, S. Daschakraborty, and R. Biswas, *J. Chem. Phys*., **140**, 104514 (2014).
36. P. Hu, R. Zhang, X. Meng, H. Liu, C. Xu, and Z. Liu, *Inorg. Chem.*, **55**, 2374 (2016).
37. M. Angell, C.-J. Pan, Y. Rong, C. Yuan, M.-C. Lin, B.-J. Hwang, and H. Dai, *PNAS*, **114**, 834 (2017).
38. A. P. Abbott, R. C. Harris, Y.-T. Hsieh, K. S. Ryder, and I.-W. Sun, *Phys. Chem. Chem. Phys.*, **16**, 14675 (2014).
39. F. Coleman, G. Srinivasan, and M. Swadźba-Kwasńy, *Angew. Chem., Int. Ed*., **52**, 12582 (2013).
40. J. Estager, P. Nockemann, K. R. Seddon, M. SwadzbaKwasny, and S. Tyrrell, *Inorg. Chem*., **50**, 5258 (2011).
41. A.P. Abbott, G. Capper, D.L. Davies, K.J. McKenzie, and S.U. Obi, *J. Chem. Eng. Data*, **51**, 1280 (2006).
42. D. Paterno, E. Rock, A. Forbes, N. Mohammad, and S. Suarez, *J. Molecular Liquids*, Accepted August 20, 2020. Publication pending.
43. C.A. Angell, *Science, New Series*, **267**, 1924 (1995).
44. B. Geĺinas, M. Natali, T. Bibienne, Q. P. Li, M. Dolle,́ and D. Rochefort, J. *Phys. Chem. C*., **120**, 5315 (2016).

45. P.M. Richardson, A.M. Voice, and I.M. Ward, *Polymer*, **97**, 69 (2016).
46. H. Shimizu, Y. Arioka, M. Ogawa, R. Wada, and M. Okabe, *Polymer*, **43**, 540 (2011).
47. W. Cui, Y. Lansac, H. Lee, S.-T. Hong, and Y. H. Jang, *Phys. Chem. Chem. Phys*., **18** 23607 (2016).
48. C.-K. Kim, K. Kim, K. Shin, J.-J. Woo, S. Kim, S.Y. Hong, and N.-S. Choi, *ACS Appl. Mater. Interfaces*, **9**, 44161 (2017).
49. C. Liu, W. Chen, Z. Wu, B. Gao, X. Hu, Z. Shi, and Z. Wang, *J. Molecular Liquids*, **247**, 57 (2017).
50. H. Shobukawa, J. Alvarado, Y. Yang, and Y.S. Meng, *J. Power Sources*, **359**, 173 (2017).
51. M. Yoshizawa, W. Xu, and C.A. Angell, *J. Am. Chem. Soc.,* **125**,15411 (2003).
52. J.P. Belieres and C.A. Angell, *J. Phys. Chem. B*, **111**, 4926 (2007).
53. S. J. Bass, W. I. Nathan, R. M. Meighan, and R. H. Cole, *J. Phys. Chem*., **68**, 509 (1964).
54. G.R. Leader and J.F. Gormley, *J. Am. Chem. Soc.,* **73**, 5731 (1951).
55. L.R. Dawson, R.H. Graves, and P.G. Sears, *J. Am. Chem. Soc.*, **79**, 298 (1957).
56. M. Zhao, B. Wu, S. I. Lall-Ramnarine, J.D. Ramdihal Papacostas, E. D. Fernandez, R.A. Sumner, C.J. Margulis, and E.W. Castner, *J. Chem. Phys*., **151**, 074504 (2019).